The Onset of Aerodynamic Instability in a 3-Stage Transonic Compressor

F.-O. Methling, R. Preute, H. Stoff
Fluid Energy Machines, IB 4-152
Ruhr-University, D-44801 Bochum (Germany)

F. Grauer
MTU (TPKE), POB 500 640
D-80976 Muenchen (Germany)

ABSTRACT

The actual research activities concerning the aerodynamic instability of compressors aim at an improvement of the usable range of the compressor performance map. Usually there must be a safety margin between operating point and stability limit to avoid stall and surge. In this paper we give a survey of the pre- and the post-instability behaviour of a 3-stage transonic axial aero-engine compressor. The measurement results of fluctuations of static and total pressure, temperature and velocity under the influence of stall and surge are presented. For that were used piezo-resistive transducers, cold wires and triple-split-film sensors. The pressure signals show, that the investigated compressor flow goes into instability by a spike-type stall.

The rotating stall frequency corresponds to nearly half of the shaft speed. The stall cell spreads at once over all three stages of the compressor and, after an oscillation at the beginning, extends approximately over a range of 1/3 to 1/2 of the circumference. Depending on the shaft speed different forms of instability occur like rotating stall, classic surge (local backflow) and deep surge (complete flow reversal).

In the second part of this paper we analyse results using fast fourier transform and artificial neural networks. It is shown, that by using the fast fourier transform peripheral disturbances can be identified, but that an artificial neural network is the most useful tool to indicate an approaching instability in case of spike-type stalling.

INTRODUCTION

In a compressor performance map the surge line is the aerodynamic stability limit towards low massflow. The different forms of those aerodynamic instabilities are rotating stall and surge. Rotating stall defines a compressor instability where regions of reduced or reversed flow occur locally whereas surge is characterized by a system instability with violent oscillations in the annulus flow throughout the compression system. Surge can be devided into two different forms, the so called *classic surge*, that means, the mass flow decreases intermittently and *deep surge* in which the mass flow becomes negative. The different forms are described in detail by e.g. Day, 1996a or Rippl, 1995.

Figure 1 shows the schematic view of a performance map of a compressor for the purpose of discussing forms of instability.

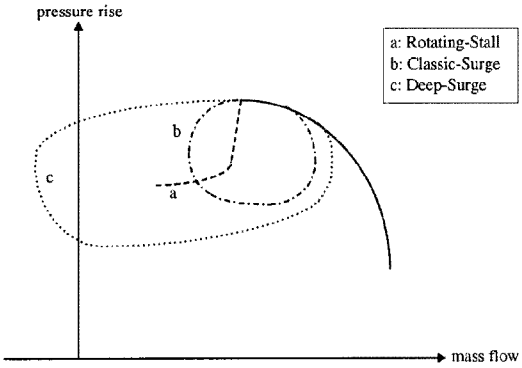

Figure 1: Compressor performance during stall and surge

All of those forms of instability are stressing the engine heavily, sometimes even leads to destruction. Strain gauge measurements in the literature report of bending stress in vanes exceeding stable operation by a factor of 2 during surge and by 5 under conditions of rotating stall (Baumann, 1970; Rippl, 1995). For this reason numerous investigations are under way to find reliable means for monitoring an eventual approach to the stability limit while running the machine (Nenni & Ludwig, 1974; Ludwig & Nenni, 1978; Day et al., 1999; Höss et al., 1998; Walbaum & Rieß, 1998). Ways for alerts have been identified for individual test beds but a reliable warning of general validity also for foreign compressor designs is still unattained (Ludwig & Nenni, 1980; Schulze u.a., 1998; Regnery, 1998; Grauer, 1998), but there is still a quest for proof of reliability fostering more research projects. Two different concepts have been devised to avoid compressor instability, known as *passive control* and *active control*.

The concept of *passive control* is related to activities to extend the usable range of operating, e.g. casing treatment. The second concept, known as *active stall control*, means to prevent the compressor from entering

Paper presented at the RTO AVT Symposium on "Active Control Technology for Enhanced Performance Operational Capabilities of Military Aircraft, Land Vehicles and Sea Vehicles", held in Braunschweig, Germany, 8-11 May 2000, and published in RTO MP-051.

unstable operation by increasing the distance to the surge line as soon as a critical approach is detected. This may be done by blow-off valves, guide vane adjustment (Day, 1991) or fuel reduction. Another concept attempts to move the surge line actively towards lower throughflow and higher pressures by the influence of actuators. Doing this enables to maintain the speed line and shifting the surge line to provide for increased operating range (Day, 1991, 1996b). For the concept of active stall control it is at first necessary to detect the approach to unstable conditions reliably.

The following sections present investigations of the onset of stall and surge in a high-speed compressor of 3 stages by using high resolution measurement techniques and in the second part results of data analysis are presented that aim to deliver a reliable technique to detect the approach to the unstable range.

EXPERIMENTAL SETUP

Compressor test rig

The 3-stage test compressor at the lab in the University of Bochum (Figure 2) is equipped with double circular arc aerofoils (DCA) in blades and NACA-65 in vanes. Its specifications are listed in table 1.

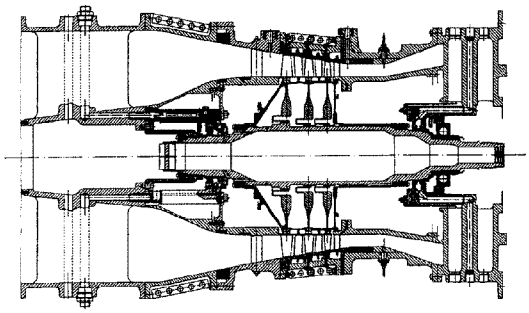

Figure 2: 3-stage compressor

As the test rig simulates the flow in the intermediate compressor of the RB 199 jet engine, the Bochum test rig is equipped with a hub spoiler (wire screen) to achieve an inlet velocity distribution similar to the discharge of the low-pressure compressor. The spoiler influences the amount of throughflow but does not change the instability phenomena in their character. For this reason the hub spoiler configuration is not varied here and all results include this influence. For closed-loop operations, the compressor is connected by rather extensive piping of more than 15 m in length equalling to a volume of 3,5 m^3 towards the inlet throttle and 5,5 m^3 towards the back-pressure throttle. The influence of the length of the piping must be the reason of a waviness of about 10 Hz superposed by disturbances from travelling waves in the piping. For conveniently isolating the different types of unstable flow regimes (during stall and surge), all tests are taken with the "large" volume (5.5 m^3), as indicated above and demonstrated on this installation by Rippl, 1995.

Compressor geometry

Rotor diameter (inlet)	494 mm
Rotor diameter (outlet)	453 mm
Hub diameter (const.)	384 mm
Hub / Tip ratio (inlet)	0.78
Hub / Tip ratio (outlet)	0.85
Aspect ratio	1.6 – 2.3
Solidity	1.2 – 0.92

Design performance data

Pressure ratio	2.67
Maximum mass flow, 100 % speed	15.1 kg/s
Relative Mach number	1.12 – 0.92
Number of revolutions	- confidential -

Compressor blading

Position	Blade type	Number of blades
IGV	NACA 65	52
Rotor 1	DCA	59
Stator 1	NACA 65	127
Rotor 2	DCA	67
Stator 2	NACA 65	159
Rotor 3	DCA	89
Stator 3	NACA 65	157

Table 1: Compressor data

Instrumentation

Data about the unsteady movement of the flow are acquired from wall-mounted pick-ups for static pressure and from traversing individually a piezo-resistive transducer for fluctuations in total pressure, a triple-split-film probe for velocity-density and flow angle as well as a cold-wire sensor for temperature. Figure 3 shows a scheme of the instrumentation.

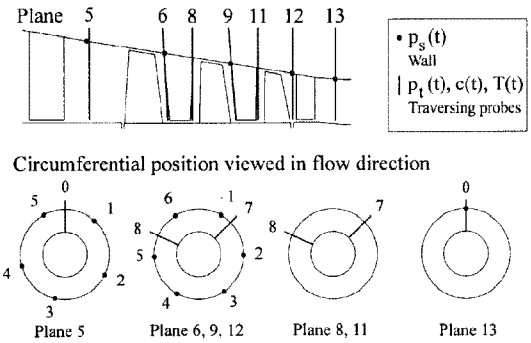

Figure 3: Instrumentation and measurement sections

As shown in figure 3 there are 5 pressure transducers in front of rotor 1 and 6 pressure transducers in front of the stators. Further it is possible to traverse sensors over the blade height in one circumferential position in front of stage 1 and behind stage 3 as well as in two different circumferential positions within the three stages.

As the bladed duct converges from a height of about 54 mm down to 34 mm, flow data are acquired only at 10 %, 50 % and 90 % of the blade span in the axial gaps

upstream of rotor 1, downstream of rotor 2 as well as of stators 2 and 3 during the occurrence of rotating stall at 50 % speed and classic surge at 60 % speed with local backflow. Speeds of 70 % and more destroy the highly sensitive wire probe due to an increased stress because of growing velocity-density. Test data have been taken with individual traversing probes in order not to obstruct the flow unduely because the pitch is going down to only 8 mm locally. The axial gaps of sizes of 5 to 6 mm restricted the probe sizes. They were of the order of 2 mm in diameter.

All transducers and probes involved in measurements of unsteady quantities enable to resolve frequencies of 1 kHz or higher (semi-conductor pressure probes 70 kHz, split-film for velocity-density 1 kHz and cold wire for total temperature 2 kHz). A low-pass filter of 10 kHz has been applied to cut off blade-passing frequencies. The instability of the compressor flow is governed by frequencies lower than the revving speed. With the exception of the total-pressure traversing probe, which is a development by Lohmberg, 1995, all other sensors (split film, cold wire) are commercially available tools. Preute, 1997, describes the calibration of the cold-wire temperature probe. The components of the measurement chain are standard equipment likewise.

With some of the signals displayed as phase averages of 4 to 5 traces, the compound effort in instability events amounts to 147 for the compressor (Preute, 2000) preceded by at least the same number of events during earlier investigations (Rippl, 1995).

RESULTS OF UNSTEADY MEASUREMENTS

Flow field results

A problem associated with measurements of the unsteady movement of the flow field is that several pick-ups for physical quantities have to be distributed throughout the flow field to capture instantaneous information in a synchronous way to reproduce a correct impression of the situation, as required e.g. for turbulence, which is considered to be a random phenomenon and cannot be reproduced in a certain moment. Unsteady movements in the flow of turbomachinery such as interacting wakes, pressure waves or stall cells can be traced in phase space with their deterministic features if it is possible to detect them. In the case discussed here an arrangement of many probes for simultaneous data acquisition throughout the flow field risks to influence the result due to blockage by the shafts of several probes. Therefore the present experiments are extracted from sequences of repeated tests with only a single traversing probe immersed in the flow field. As the phenomena of unstable flow occur rapidly, there is no time for traversing the probe over the channel height.

Separate test runs have to be performed for each measurement location. Synchronisation of the events is achieved by triggering on ramps of stall or surge events over the elapsed time or the position of the shaft. In this way characteristic pattern in the signals may be enhanced by phase-averaging several events if a single signal is blurred by random motion. 6 flush-mounted wall-pressure probes, which do not obstruct the cross section of the flow, measure simultaneously in distributed positions in the wall of the casing. Wall pressure signals measured in section 5 upstream of rotor 1, shown in figures 4 and 5, reproduce the distinctly different forms of instabilities as they have been found by Rippl (1995) for the setting of velocity and backpressure throttle: Rotating stall occurs at 50 % rated speed where flow reversals take place only locally near blades and vanes (top of figure 4).

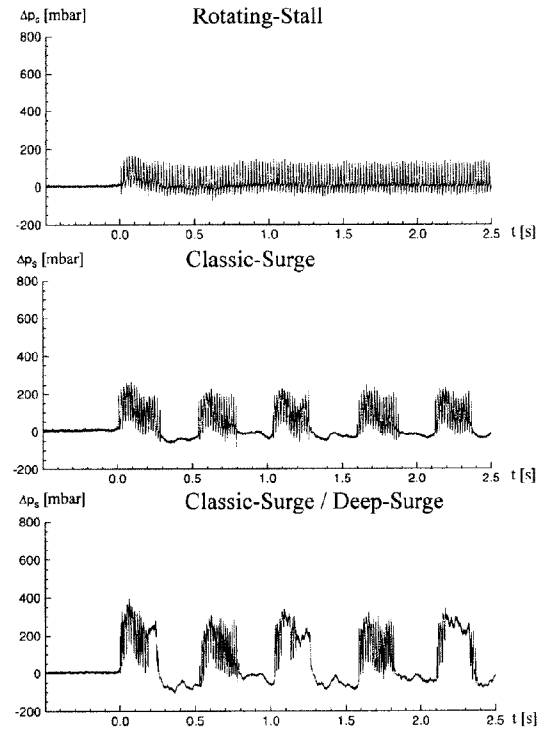

Figure 4: Static pressure in front of rotor 1 (section 5) during transition from stable to unstable flow for rated speeds of 50 % (rotating stall, top), 60 % (classic surge, middle) and 70 % (intermittent classic surge and deep surge, bottom).

The so-called "classic surge" with momentary flow reversal in single rows appears on the operating line of 60 % rated speed in the compressor map when throttling brings the operating point over the limit of stability. The integral mass flow is still through the outlet (Figure 4, centre).

At 70 % rated speed (Figure 4, bottom) a transitional form of instability takes place, changing alternately between classic surge and deep surge, occasionally reversing the flow.

At 80 %, 90 % and 100 % rated speed excessive throttling produces flow reversal alternately emptying the back-pressure piping and consecutively recovering the back-pressure in the outlet. The latter flow regimes may be reached only with inlet throttling because of power limits in the transmission gear. The results in figure 5

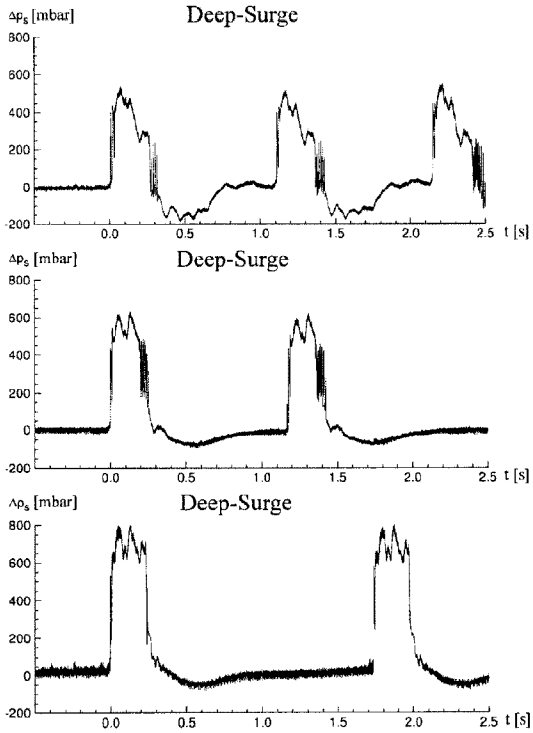

Figure 5: Static pressure in front of rotor 1 (section 5)during transition from stable to unstable flow for rated speeds of 80 %, 90 % and 100 % showing deep-surge with flow reversal during static pressure rise.

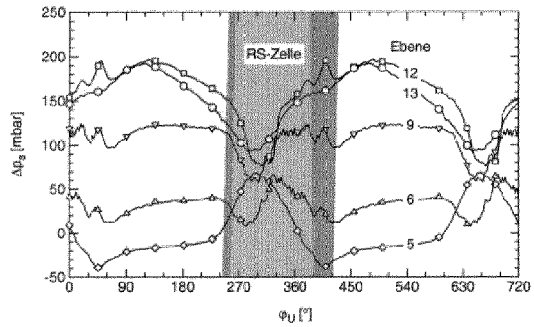

Figure 6: Measurements of wall pressure in the sections 5, 6, 9, 12 and 13 extending peripherally along the circumference. Within the domain of the stall cell the pressure drops in the rear stages and overshoots ahead of rotor 1.

verify the reproduceability of the situations encountered by Rippl (1995) during preceding tests. The flow regimes of rotating stall at 50 % and of classic surge at 60 % rated speed proved to be accessible to the equipment of measuring distributions of velocity-density and total temperature. Flow conditions at 70 % rated speed and above wiped out the high sensitivity temperature transducer (cold wire of 2.5 μm) and requires other dispositions for the velocity-density measurement due to high temperature levels.

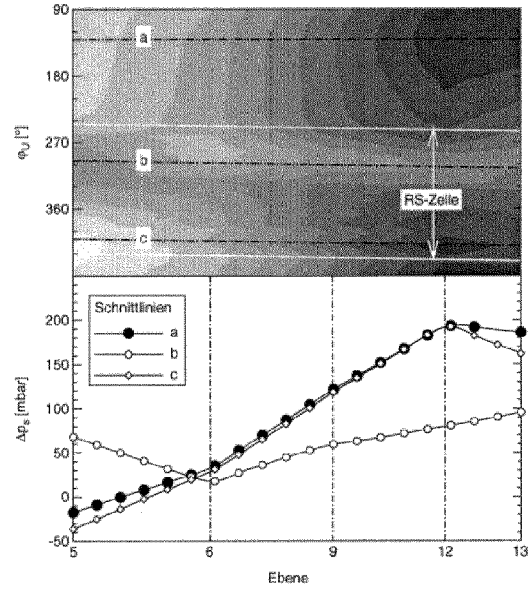

Figure 7: Static pressure Δp_s along 3 circumferential positions φ_u on the casing wall showing the axial distribution under the influence of a stall cell. A S2 computation by ZORBA2 (Novak, 1966) matches with distribution a (- ● -)

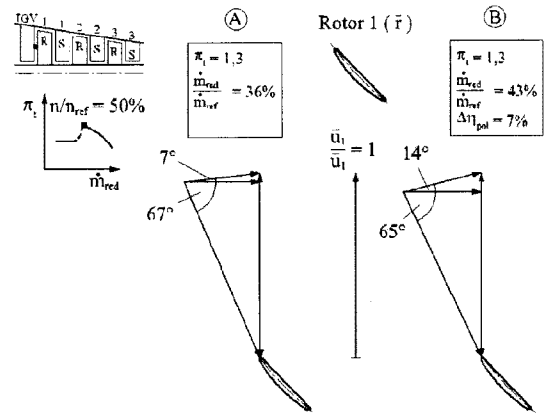

Figure 8: Velocity triangles in the aerodynamically stable range near the stall limit at 50 % rated speed and mid-height in front of rotor 1: - A) computed from measurements; - B) taken from a S2 computation (Novak, 1966)

Figure 6 displays the peripherally distributed pressure pattern for the sections at 50 % speed collectively. The development of pressure over the stages is displayed in figure 7 at one instant showing the rise and fall of pressure for 3 selected peripheral positions of which one is affected by the travelling stall cell. Comparison with a time-independent off-design S2 computation with the

axisymmetric streamline-curvature method ZORBA2 (Novak, 1966) show the flow to compare well with quasi-steady conditions in moments where flow recovery returns. It should be mentioned here that Rippl (1995) found out that the mean swirl angle of the flow leaving the inlet guide vane varies between 4° and 10° with the chord Reynolds number and the computation used the vane angle of 14°. The Carter turbine rule (Hawthorne, 1964) yields 6° of deviation, i.e. 8° for the flow angle.

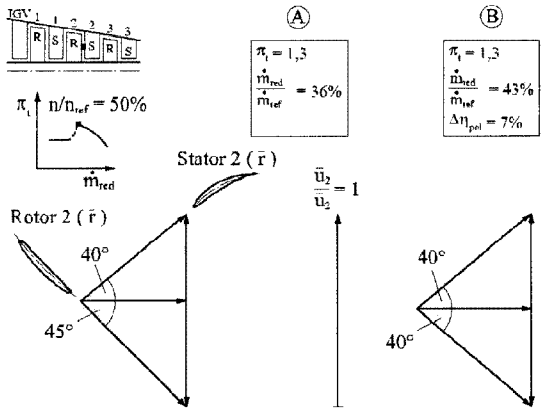

Figure 9: Velocity triangles in the aerodynamically stable range near the stall limit at 50 % rated speed and mid-height in front of stator 2:
- A) computed from measurements;
- B) taken from a S2 computation (Novak, 1966)

But as the S2 computation does not rely on the measurement, a discrepancy remains here. The results at 50 % rated speed presented hitherto (figures 8, 9) originate from an operating point on the 50 % speed line which, when crossing the limit of stability, drops in total pressure ratio from $\pi_t = 1{,}3$ to $\pi_t = 1.2$ with a mass flow decrease from 36 % to 27 % due to local flow reversal (figure 10).

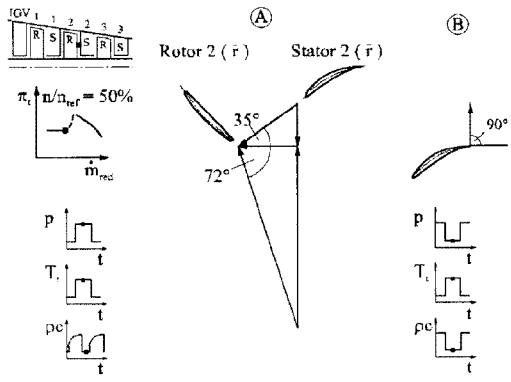

Figure 10: Velocity in the aerodynamically unstable range at 50 % rated speed and mid-height:
- A) The moment of local backflow in front of stator 2 computed from measurements;
- B) The moment of cirumferential flow at the trailing edge of stator 2 from figures 11, 12

The velocity triangle (figure 10) is computed from measured data, see figures 11 and 12.

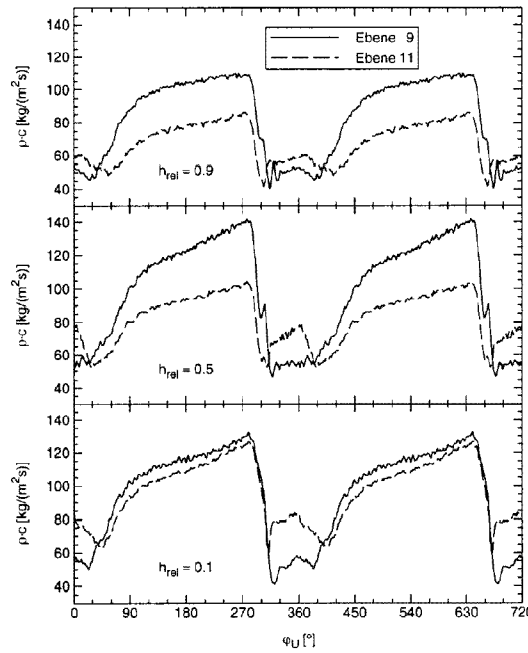

Figure 11: Distribution of the modulus of the velocity-density over the peripheral direction at 10 %, 50 % and 90 % height of the channel in front of stator 2 (section 9: —) and behind stator 2 (section 11: - - -) at 50 % rated speed

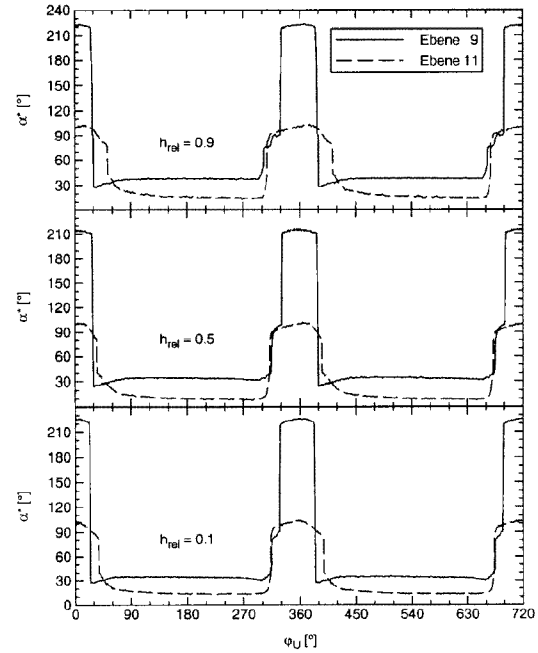

Figure 12: Distribution of flow angle over the peripheral direction at 10 %, 50 % and 90 % height of the channel in front of stator 2 (section 9: —) and behind stator 2 (section 11: - - -) at 50 % rated speed

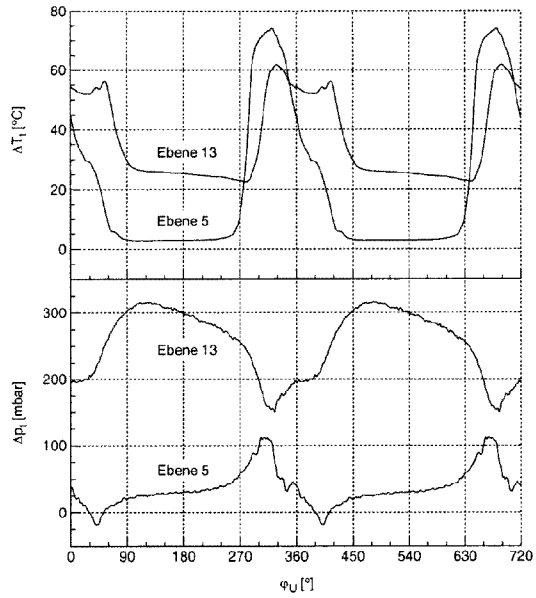

Figure13: Distributions of wall pressure and total temperature over a sector of the blading before the first (section 5) and after the last stage (section 13) during rotating stall at 50 % shaft speed and mid-height

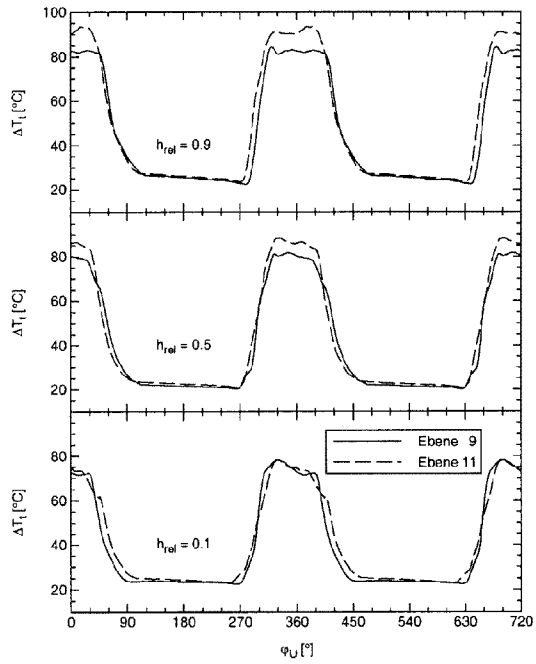

Figure 14: Distribution of total temperature over the peripheral direction at 10 % (bottom), 50 % (middle) and 90 % (top) height of the channel in front of stator 2 (section 9: —) and behind stator 2 (section 11: - - -) at 50 % rated speed

In this situation it is interesting to see how, during moments of stall, the wall pressure drops over a sector of about 120° in a row at the rear end of the blading. During that time the pressure rises in front of the blading as the local recirculation jams the flow through this peripheral sector (figure 13). A rise of the total temperature to 2 to 3 times the stable level goes along with the drop in the backpressure and the burst in front of the blading. By estimating the continuous energy input from the shaft at constant speed, it can be estimated that the amount of energy supplied, reduced by the energy requirement for the remaining through flow, is high enough to bring the air enclosed in the volume of the stall cell to such a temperature as measured here (figure 14).

The volume of the stall cell spreads over 1/3 (Rippl, 1995) to 1/2 (Preute, 2000) of the blading (figure 15). The strong increase in temperature observed here is confirmed by other observations in which blade failures during stall can be clearly attributed to overheating as their colour turned to blue (Strub & Suter, 1965) or the blading melted away (Hoffeins et al., 1980).

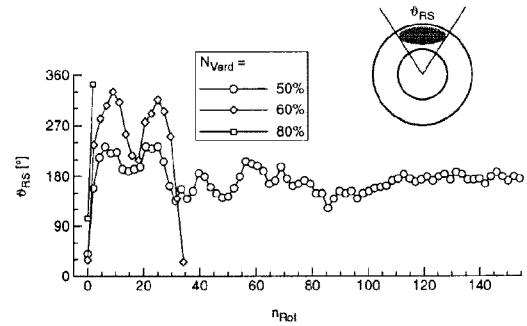

Figure15: Peripheral extension of the stall cell over the number of revolutions of the shaft for rated speeds of 50 % (- o -), 60 % (-◇-) and 80 % (-□-)

The measured unsteady results appear to be plausible when compared in a quasi-steady manner to S2 data from a streamline-curvature method which had been adjusted for the target pressure ratio by input of a corresponding mass flow, without tuning deviation and loss to fit efficiency and through flow to the experiment. The pressure rise in figure 7 as well as the velocity triangles in figures 8, 9, 16 and 17 support the measured results.

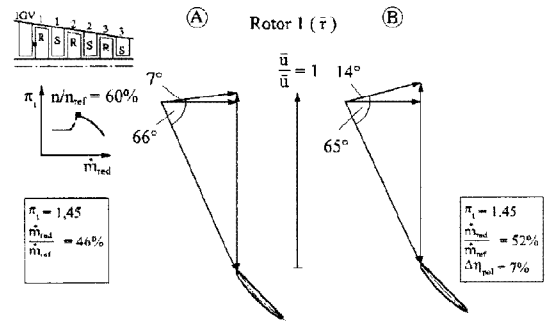

Figure 16: Velocity triangles in the aerodynamically stable range near the stall limit at 60 % speed and mid-height in front of rotor 1:
- A) computed from measurements
- B) taken from a S2 computation (Novak, 1966; ZORBA2)

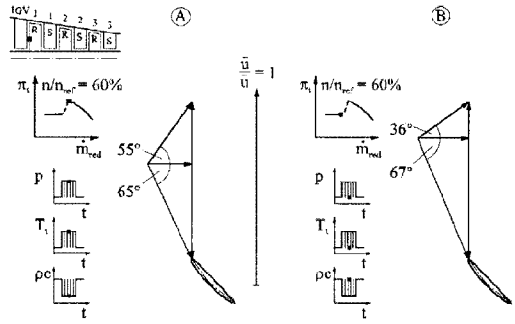

Figure 17: Velocity triangles for intermittent flow of classic surge at 60 % rated speed and mid-height in front of rotor 1:
- A) moment of minimum through flow:
- B) moment of maximum through flow

Keeping in mind that the electric power drops by up to 10 % when entering stall at 50 % speed from the primary characteristic (π_t = 1,3; $\dot{m}$ = 5,5 kg/s) to the secondary characteristic (π_t = 1,2; $\dot{m}$ ≈ 4,2 kg/s), then the power requirement would drop to half its value.

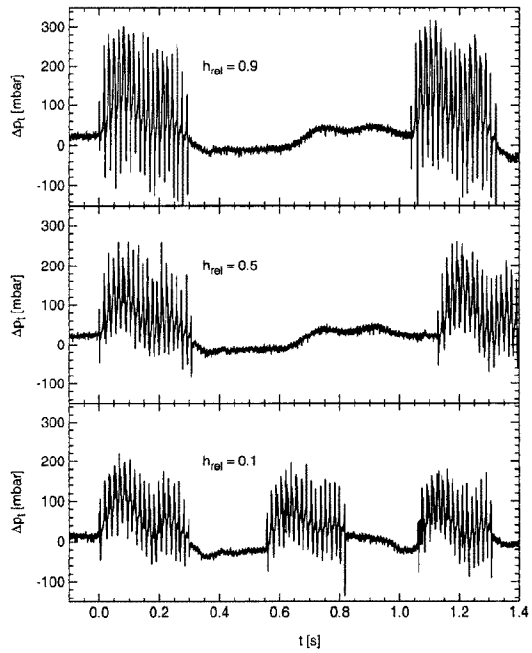

Figure 18: Distribution of total pressure over the time for 10 %, 50 % and 90 % height of the channel at 60 % rated speed in front of rotor 1 (section 5)

If the same efficiency applies, then about 40 % of the shaft power enters the air and heats up 5,5 kg/s – 4,2 kg/s = 1,3 kg/s of mass flow recirculating in the cell, which brings the temperature inside the stall cell up to approximately 50 °C whereas 20 °C to 30 °C would be the temperatures associated with an adiabatic compression for pressure ratios of π_t = 1,2 to 1,3. Similarly to 50 % speed, at 60 % speed the total temperature rises to more than 100 °C whenever local detachment of flow occurs with the flow angle snapping from 7° to about 50°, the speed falling to less than half the stable level and the pressure shooting up in front of the blading (figures 18, 19, 20).

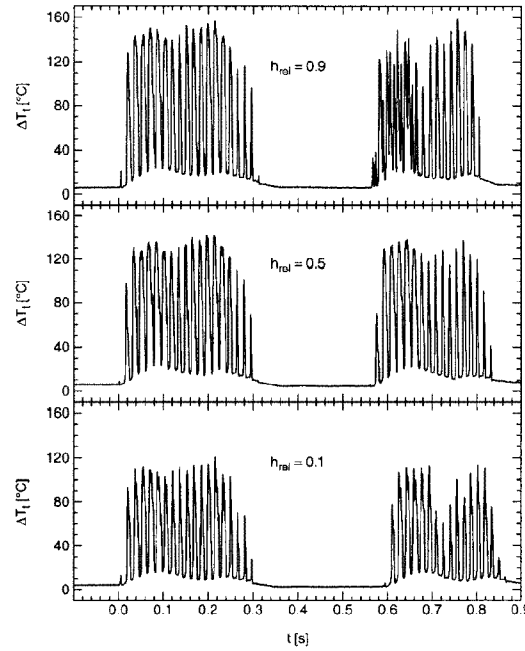

Figure 19: Distribution of total temperature over the time for 10 %, 50 % and 90 % height of the channel at 60 % rated speed in front of rotor 1 (sec. 5)

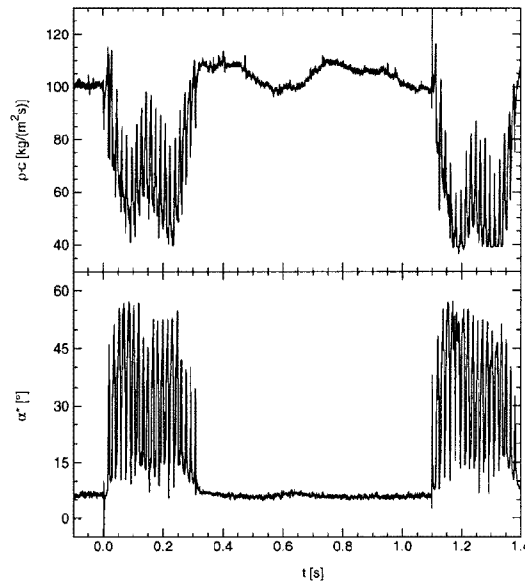

Figure 20: Distributions of the modulus of the velocity-density and the flow angle over the time at 60 % rated speed and mid-channel in front of rotor 1 (section 5)

When approaching the situation of stall, it is not easily possible to recognize the appearance of precursor wave patterns at a time sufficiently large to allow for

preventive action. Figure 21 shows the signals as acquired from the measurement beginning about 4,5 revolutions ahead of the stall event. First disturbances show only ½ revolution before stall. A precursor wave information serving as a stall detector cannot be discerned sufficiently early without special analysis of the signal, as will be shown below.

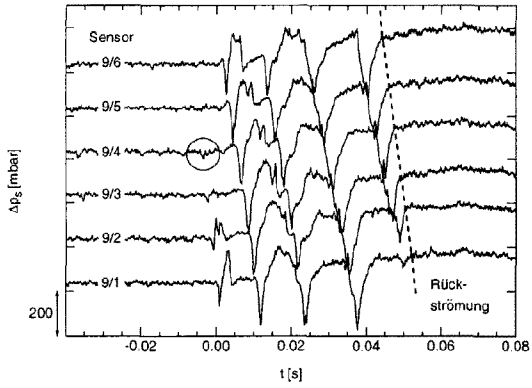

Figure 21: Distribution of wall pressure over the time for 6 transducers mounted peripherally in the casing in front of stator 2 (section 9) at 50 % rated speed. The trace of the signal starts about 40 ms, i.e. 4.5 revs., ahead of the first visible indication of stall.

RESULTS OF DATA ANALYSIS

As mentioned above, first it is necessary to detect the approach of the compressor operating point to unstable conditions before developing a control system to avoid this. Therefore different analysis techniques were developed and tested at the University of Bochum which aim at a reliable detection of reaching unstable regions of the compressor performance map. An extensive database was taken to compare data of the stable region to data nearby the surge-line at different speeds. The database for the analysis is given in figure 22.

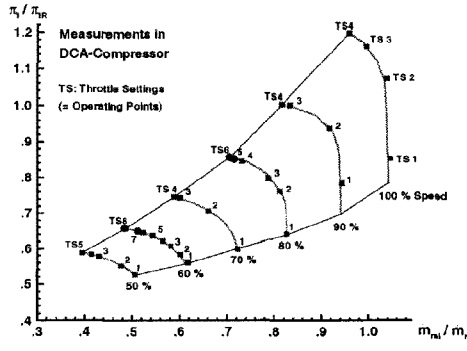

Figure 22: Database

The static pressure was recorded at 5 different circumferential positions in front of rotor 1, see fig. 3. The results of the analysis are given in the following sections.

Circumferential Fourier-Transform

This method takes advantage of the circumferentially distributed pressure transducers. The spatial Fourier-transform provides information about the amplitude and the phase of a peripheral pressure fluctuation. By calculating the change in phase between each time step, information about the rotational speed of the disturbance can be extracted. Another way to uncover rotating perturbations from the data has been described by Tryfonidis et al. (1994). Further explanations about these techniques are given by Grauer (1998). The time-dependent behaviour of these rotating perturbations can be observed by introducing a time window, which is shifted along the complex result of the first Fourier-transform.

The results of this analysis show, that there exist frequency ranges, where the amplitudes grow when the working line approaches the stability limit. One criterion for a stall warning can be figured out by integrating the amplitudes within a frequency band between 20 % and 50 % of the rotor frequency (Grauer, 1998).

Figure 23 displays the results for the 60 %, 80 % and 100 % speed of the compressor by comparing the sum of amplitudes which means the intensity of rotating disturbances.

Figure 23, at left, shows the results for a working point in the stable region and, at right, for a working point approaching the surge line. It can be seen, that there is a clear increase of the amplitudes.

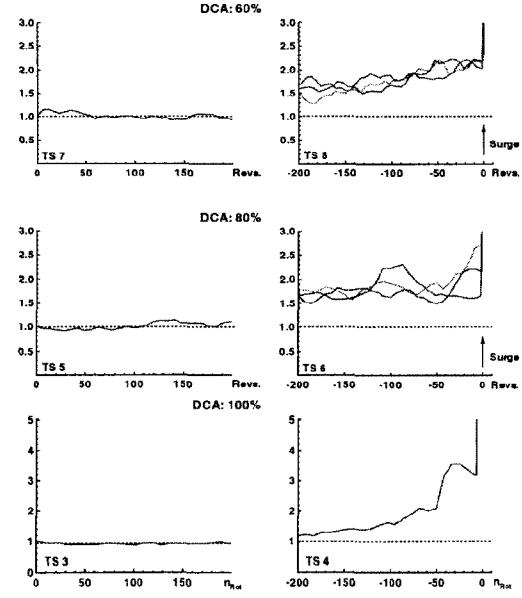

Figure 23: Intensity of rotating disturbances

For the application of this analysis technique, the signals of at least 3 pressure transducers are necessary, because the presented results were calculated from the first harmonic of the spatial Fourier-transform. The data of the

measurement section in front of rotor 1 were taken because earlier investigations have shown, that the best results were obtained from the signals of the transducers installed in front of the first stage (Grauer, 1998). Stage matching and hence the axial location of the onset of stall did not play an important role for this investigation. This may be due to the comparatively small length of this compressor.

Grauer (1998) has found out by investigating data of different compressors, that this behaviour is typical and can be used in a compressor control system to detect the approach to unstable conditions. A great disadvantage of this technique is, that it needs a minimum of three transducers over the compressor circumference, to calculate the Fourier-transform.
The described calculations not only deliver a criterion easy to obtain for a stall warning, they furthermore give a deeper insight into the characteristics of the signal during the stall inception process, which is helpful for the development of other analysis techniques to reduce data processing and instrumentational effort. One of these techniques, which centres on the observation of the rotor-speed periodic disturbances, is based on artificial neural networks and will be described below.

Classification using Artificial Neural Networks
Artificial neural networks attempt to imitate the biological brain in technical applications in the fields of pattern recognition and control. They can be adapted to a variety of problems and are able to extract information from data submerged in noise. Their capability goes beyond a simple analysis of the data as they can also serve for purposes of control

Figure 24 shows the basic elements of a neural network. It consists of many non-linear computational elements called nodes (represented by rectangles in figure 24) which are connected by links of variable weights. Data that have to be processed by the network reach the net via an input layer and are transmitted to the following layers by the weighted links. Basics about neural networks can be found in the literature (for example: Ritter et al., 1991; Zell, 1994).

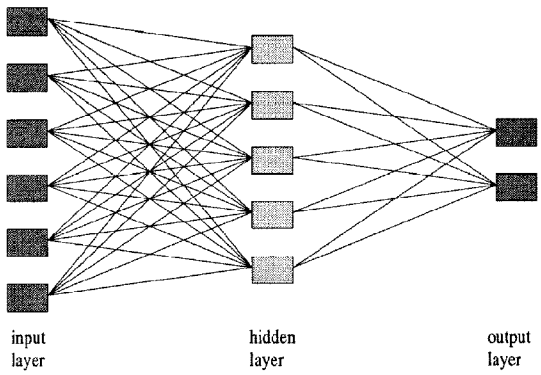

Figure 24: Basic elements of neural networks

Working with a neural network first requires adapting the net to the special problem. This is done during a separate process called the learning or training phase. One of the methods most frequently used is called *supervised learning*, which means that representative data, which describe the problem as detailed as possible, are presented to the net together with the respective output. The learning process is finished, if the calculated error between the network output and the teaching output reaches a given tolerance margin.

The presented results were obtained by the *Stuttgart Neural Network Simulator* (SNNS) which is developed at the *Institute for Parallel and Distributed High Performance Systems* (IPVR) of the University of Stuttgart, Germany. The simulator consists of various network types and other variable parameters. For the following investigations a feedforward net and the *cascade correlation learning algorithm* was used (Zell, 1994), as this combination yielded the best results.

Every neural network will work as well as the data, which were presented during the learning period, describe the problem to be handled. Therefore, apart from a good choice of network models, connection types and learning rules, which all have a significant influence on the network's performance, the most important step is to extract clear sets of data (called *input pattern*). Measured data can be improved by appropriate preprocessing, which can be achieved by different analysis techniques. As described in the former section, rotor-speed periodic disturbances were found in the pressure signal, that changed during stall inception.

Different analysis techniques gave a detailed insight into the structure of the pressure fluctuations. Referring to figure 23 a difference between the throttle settings 1-7 (60%), 1-5 (80%) or 1-3 (100 %) to those settings representing the stall inception [TS 8 (60%), TS 6 (80%) and TS 4 (100%)] was clearly indicated for example by the circumferential Fourier-transform described in the former section. As these differences should also be visible in the untreated pressure signals, they were observed in detail to find out comparable structures.

To remove noise, the signal was ensemble averaged over 10 rotor revolutions and then observed over a time of about one rotor revolution. The signals were normalised in an interval of [0,1] for each throttle setting, so differences due to the absolute pressure value were avoided. The length of the generated pattern covers an interval of 50 samples which means nearly one rotor revolution. The way of input pattern generation from the pressure signal is given in figure 25.

This generating of input pattern for the neural network has been done for all different speeds of the compressor. The network was trained and tested with the data of sensor 4. The validation has been done by using data

from different sets of measurements. The network generated with those data is given in figure 26. The output-layer design of the network belongs to the different compressor speeds.

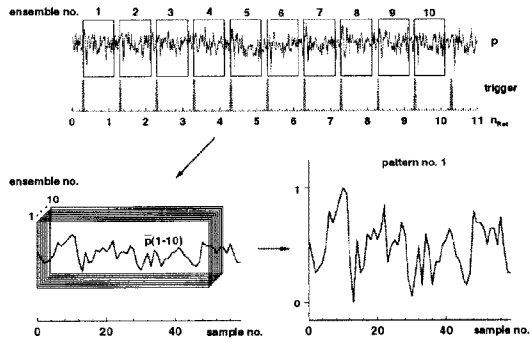

Figure 25: Generation of input pattern

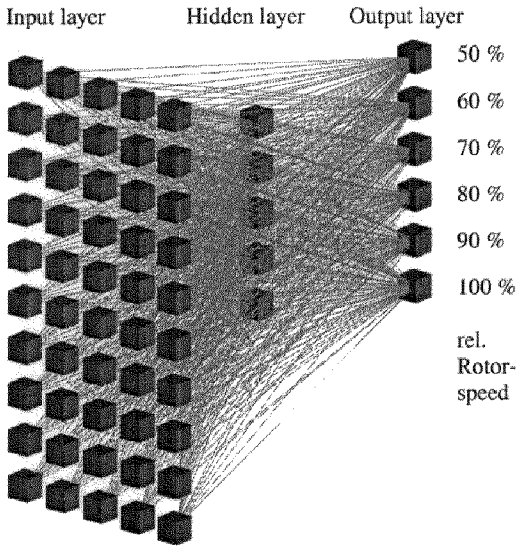

Figure 26: Neural Network after training

The teaching output of the network was 0.3 for regions of stable operation and 1.0 for operating points that are approaching the surge line. Fig. 27 displays the results of data classification using the network shown above (figure 26) with the "unknown" testdata put into the network.

Figure 27 displays an example of the network output for each compressor speed. One or two datasets are from a stable operating range (S#) and the other output (TR) comes from a dataset approaching the surge line. As it can be seen, the network output does not exactly correspond to the teaching output (defined before as 0.3 or 1.0) but it can clearly be decided between stable and unstable compressor operation by using such an artificial neural network.
Due to the high-speed data acquisition of transient data, this behaviour of the network output is expected.

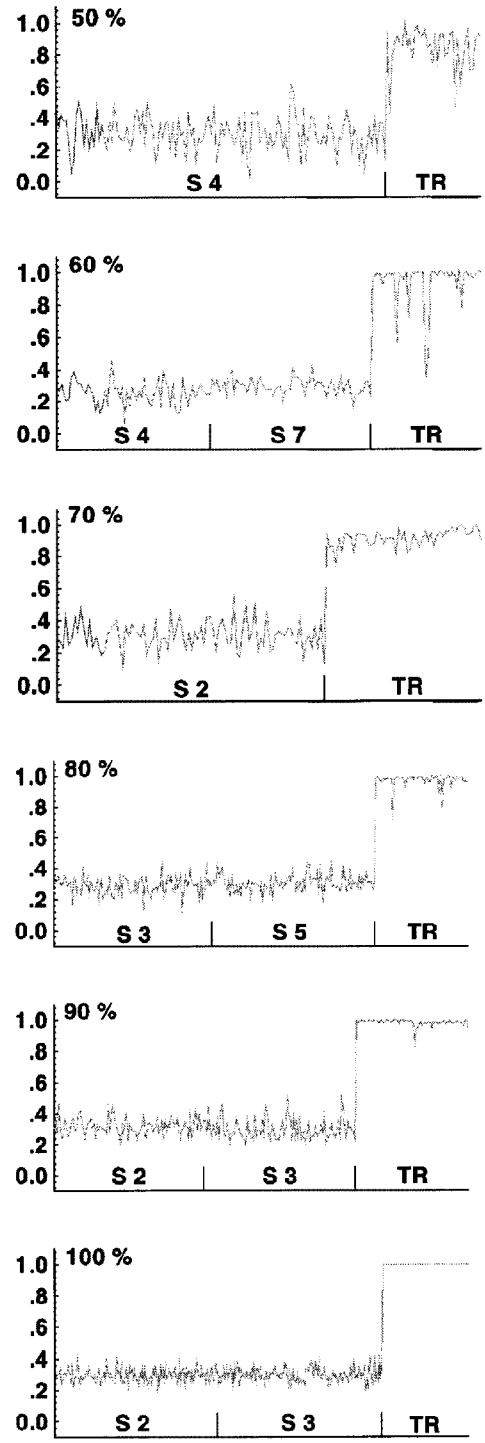

Figure 27: Network output of the different output nodes belonging to the individual rotor speeds

It is impossible to eliminate all noise of the signal by ensemble averaging. Nevertheless the network output is unambiguous if it is interpreted e.g. by a decision as "less than 0.5" or "greater than 0.7".
By analysing the network output in this way it can be stated that with the exception of 2 input patterns at rated speed of 50 % and 3 input patterns at rated speed of 60 % all input pattern are classified correctly. If the decision

between stable and unstable compressor operation is then based on taking e.g. 3 following networkoutputs, the system is absolutely reliable.

This result shows that a stall warning based on this network produces a warning in time. Nevertheless it is possible to improve the performance by treating more data during the learning process, which can easily be obtained by further measurements. Such measurements are planned in the future to investigate the performance of the described method over the whole speed range and with repeated stall events.

The described method centres on the observation of the disturbances being periodic with the rotor speed. Those disturbances can be found in compressors with a spike-type stall and in those with modal waves (Day et al., 1997). It should be possible to apply this method to both types of onset of instability. This will be a subject for investigations in the future.

CONCLUSIONS

Single-probe measurements of total temperature and velocity-density vector in front of rotor 1, behind rotor 2, stator 2 and stator 3 have been acquired at 10 %, 50 % and 90 % height of the channel at revving speeds of 50 % and 60 % of the operating range. Through the use of split-film and cold-wire probe, flow-field data with a resolution of 1 kHz in time are available to validate computer codes for unsteady simulation of unstable compressor flow situations of rotating stall and classic surge.

Steady-state streamline-curvature S2 computations have been compared to quasi-steady situations of the time-dependent flow measurements confirming the validity of velocity triangles. In this way, future measurements of high resolution in time with a direction-dependent total pressure miniature probe (2.2 mm axial extension) are enabled in axial gaps inside the stages during selected instants of time.

Unsteady measurements of wall pressures in the casing in front of the stages and at the exit as well as behind each rotor complement the temperature measurements to determine the density.

Peaks in the temperature measurement during moments of stalled flow grow to levels of 2 to 3 times the corresponding values at the same speed in the aerodynamically stable range. An energy balance estimation with the input of shaft power into locally enclosed volumes of recirculating stall cells support the temperature levels measured here.

The unsteady distributions of pressure signals over time allow to recognise precursor waves not more than about 1 revolution (approx. 5 to 10 milliseconds) prior to stall. The signal analysis using Fourier-Transforms has shown to extend the available warning time to the order of a second (i.e. 300 revs) and artificial neural networks to more than 3 seconds (800 revs) prior to stall.

ACKNOWLEDGEMENTS

The stall and surge measurements on the compressor rig at the University of Bochum were supported by the German Ministry of Education and Research (BMBF) together with MTU during the project "AG TURBO – Turbotech" under grant no. 0327041C. The signal treatment was funded by MTU during project "Engine 3E". R. Stromberg and the workshop members of the Energy Institute contributed to operation and maintenance of the test rig, D. Becker to the electronic chain of instrumentation, Mrs. M. Regulski, O. Narin and J. Schäfer to the lay-out of text and graphics. The S2 computations were put at our disposal by P. Mertes and by M. Schwarz from DEMAG. We gratefully acknowledge all these contributions.

REFERENCES

Baumann, H., 1970: "Messungen der Schaufel-beanspruchung von Axialgebläsebeschaufelungen bei rotierender Ablösung", Schweiz. Bauzeitg. 88 (11. Juni 1970)24, 541-543

Breuer, T., Servaty, S., 1995: "Stall Inception and Surge in High Speed Axial Flow Compressors", AGARD CP-571 pp. 26/1-17

Breuer, T., 1996: "Compressor Flow Instabilities: Part I: Multistage Environment, Modelling Approaches; Part II: Analysis Techniques", see VKI

Day, I.J., 1991: "Active Suppression of Rotating Stall and Surge in Axial Compressors", ASME 91-GT-87

Day, I.J., 1996a: "The Fundamentals of Stall and Surge in Axial Compressors", see VKI

Day, I.J., 1996b: "Stall and Surge in High Speed Compressors and the Prospect for Active Control", see VKI

Day, I.J. et al., 1997: "Stall Inception and the Prospects for Active Control in four High Speed Compressors", ASME 97-GT-281, Journal of Turbomachinery 121 (Jan. 1999)1, 18-27

Grauer, F. et al., 1998a: "Detection of Precursor Waves announcing Stall in two 3-Stage Axial Compressors", ASME 98-GT-520

Hawthorne,W.R., 1964: "Aerodynamics of Turbines and Compressors", Princeton Univ.Press

Hoffeins, H. et al., 1980: "Die Inbetriebnahme der ersten Luftspeicher-Gasturbinengruppe", Brown Boveri Mitt. Vol. 67 (August 1980)8, 465-473

Höss, B. et al., 1998: "Stall Inception in the Compressor System of a Turbofan Engine", ASME 98-GT-475, Journal of Turbomachinery 122 (Jan. 2000)1, 32-44

Lohmberg, A., 1995: "Entwicklung einer Sonde zur Messung flukturierender Druckspannungen im Axialverdichter", Interner Bericht, Ruhr-Universität

Bochum, Lehrstuhl für Fluidenergiemaschinen (AN99-008)
Ludwig,G.R.; Nenni,J.P., 1978: "A Rotating Stall Control System for Turbojet Engines", ASME 78-GT-115; Journal of Engineering for Power 102(Jul1979)3, 305-314
Ludwig,G.R.; Nenni,J.P., 1980: "Tests of an improved rotating stall control system on a J-85 turbojet engine", ASME 80-GT-17; Journal of Engineering for Power 102(Oct.1980)4, 903-911
Nenni, J.P., Ludwig, G.R., 1974: "A Theory to predict the Inception of Rotating Stall in Axial Flow Compressors", AIAA-74-528, AIAA 7th Fluid Plasma Dynamics Conf.
Novak, R.A., 1966: "Streamline Curvature Computing Procedures for Fluid-Flow Problems", ASME 66-WT/GT-3, Journal of Engineering for Gas Turbines Power 89 (October 1967)4, 478-490
Preute, R. et al., 1997: "Sensoren für Strömungsinstabilitäten am Beispiel eines Axialverdichters", tm – Technisches Messen 64 (Juni 1997), 238-246
Preute, R., 2000: "Experimentelle Untersuchung der aerodynamischen Instabilität in einem mehrstufigen transsonischen Axialverdichter", Dissertation, Ruhr-Universität Bochum (expected 2000)
Regnery, D., 1998: "Development of a System for the Observation of the Stable Operation in Multistage Axial Compressors", VDI-Ber. Nr.1425, 199-210.
Rippl, A., 1995: "Experimentelle Untersuchungen zum instationären Betriebsverhalten an der Stabilitärsgrenze eines mehrstufigen transsonischen Verdichters", Dissertation, Ruhr-Universität Bochum
Ritter, H. et al., 1991: "Neuronale Netze", Addison Wesley Publishing Company
Schulze,R. et al., 1998: "Experimental Examination of an Axial Compressor as a Basis for an Active Stall Avoidance System", ISROMAC-7 Paper, 22-26 Feb.1998, Honolulu, ev.IJRM Intern.Journal of Rotating Machinery
Schwarz,M., 1990: "Berechnung der Strömung und der Seitenwandgrenzschichten in mehrstufigen Axialverdichtern unter besonderer Berücksichtigung der Randzonenkorrektur", Dissertation, Ruhr-Universität Bochum
Strub, R.A., Suter, P., 1965: "Compressor Surge in Gas Turbines and Blast Furnace Compressor Installations", ASME 64-GTP-5, Journal of Engineering for Power 87(April 1965)2, 193-196.
Tryfonidis, M. et al., 1994: "Pre-Stall Behaviour of Several High-Speed Compressors", ASME 94-GT-387
Walbaum,M., Rieß,W., 1998: "Einfluß der Leitschaufelverstellung auf die Entwicklungsformen des Rotating Stall in mehrstufigen Verdichtern", VDI-Ber. Nr.1425 (1998) 177-188.
VKI LS 1996-05 "Unsteady Flows in Turbomachines"
Zell, A., 1994: "Simulation Neuronaler Netze", Addison Wesley Publishing Company

PAPER -8, F. O. Methling

Question (W. Reiss, Germany)
Do you think that this early warning method is a general solution to the problem?

Reply
The neural net method has to be trained for each machine, but seems to be quite capable.

Question (H. Weyer, Germany)
Please comment on the reasons for the sawtooth type of total pressure distribution of the first rotor.

Reply
The total pressure probe that was used, similar to a Pitot probe, is only in one particular direction which is sensitive to the total pressure. Due to the flow angle within the stall cell (see figure 12 of the paper), such a total pressure distribution can be explained.